Scientific
Research
Publishing

Dynamic Behavior Induced by the Cooperation between Two Different Ionic Conductances in a Mathematical Model of Vibrissa Motoneurons

Takaaki Shirahata

Institute of Neuroscience and Kagawa School of Pharmaceutical Sciences, Tokushima Bunri University, Sanuki, Japan
Email: tshi@kph.bunri-u.ac.jp

Abstract

A mathematical model of vibrissa motoneurons (vMN), which has been developed by Harish and Golomb, can show repetitive spiking in response to a transient external stimulation. The vMN model is described by a system of nonlinear ordinary differential equations based on the Hodgkin-Huxley scheme. The vMN model is regulated by various types of ionic conductances, such as persistent sodium, transient sodium, delayed-rectifier potassium, and slow ionic conductances (e.g., slowly activating potassium afterhyperpolarization (AHP) conductance and h conductance). In the present study, a numerical simulation analysis of the vMN model was performed to investigate the effect of variations in the transient sodium and the slow ionic conductance values on the response of the vMN model to a transient external stimulation. Numerical simulations revealed that when both the transient sodium and the AHP conductances are eliminated, the vMN model shows a bistable behavior (*i.e.*, a stimulation-triggered transition between dynamic states). In contrast, none of the following induce the transition alone: 1) elimination of the transient sodium conductance; 2) elimination of the AHP conductance; 3) elimination of the h conductance; or 4) elimination of both the transient sodium and the h conductances.

Keywords

Mathematical Model, Numerical Simulation, Vibrissa, Ionic Conductance, Bistability

1. Introduction

Neurons are examples of nonlinear dynamical systems, and their dynamics is investigated by various types of mathematical models based on the Hodgkin-Huxley equations [1]. As an example of such mathematical models, a vibrissa motoneuron model (vMN model) has been proposed [2]. This model is described by a system of non-linear ordinary differential equations (ODEs) and comprises several voltage-dependent ionic conductances: the transient sodium conductance, the persistent sodium conductance, the delayed-rectifier potassium conductance, and three types of slow ionic conductances (the slowly activating potassium afterhyperpolarization (AHP) conductance, the hyperpolarization-activated h conductance, and the potassium M conductance) (see Methods in ref. [2]). The vMN model shows various types of interesting dynamical behavior, such as repetitive spiking [2], mixed-mode oscillations [3], and bistability, between resting and spiking states [3]. It is important to understand the relationship between the ionic conductance and various dynamical behaviors of the vMN model, and several results that reveal such relationships have been reported so far, for examples, the transient sodium conductance (but not the persistent sodium conductance) is essential for generating repetitive spiking [4]; the frequency of repetitive spiking is modulated by the AHP conductance and the h conductance [2], the h conductance is involved in mixed-mode oscillations [3], and the h conductance and the M conductance are involved in bistability between the resting and spiking states [3].

Investigation of the effect of simultaneous variations in several ionic conductance values on the dynamical behavior of neuron models has been extensively performed not only in the vMN model [4] but also in other neuron models [5]-[9]. For example, the analysis of simultaneous variations in transient and persistent sodium conductances has revealed that in the vMN model, the former conductance plays a more important role in generating repetitive spiking than the latter [4]. However, the analysis of simultaneous variations in sodium and slow ionic conductances has not been performed in detail in the vMN model. Investigation of this issue may contribute to a detailed understanding of the relationship between the ionic conductance and dynamical behavior of the vMN model. Therefore, in the present study, a computer simulation analysis of the vMN model was performed to investigate the effect of variations in the transient sodium and the two types of slow ionic conductance (the AHP conductance and the h conductance) on the dynamical behavior. (In the vMN model, there are two types of sodium conductance. However, since the transient sodium conductance is considered to be more important than the persistent sodium conductance [4], the present study focuses only on the transient sodium conductance. In addition, to make the vMN model simpler, the present study does not consider the M conductance).

2. Materials and Methods

The present study performed numerical simulation of the vMN model, which is described by a system of nonlinear ODEs. As the detailed explanations of the vMN model have been given previously [2], we describe the vMN model only briefly here. The equations describing the vMN model are as follows:

$$\frac{dV}{dt} = I_{app} - g_{Na}\left(\frac{1}{1+e^{-(V+28)/7.8}}\right)^3 h(V-55) - g_{AHP}u(V+90) - g_h r(V+27.4)$$
$$-0.04\left(\frac{1}{1+e^{-(V+53)/5}}\right)(V-55) - 20n^4(V+90) - 0.12(V+70) \tag{1}$$

$$\frac{dh}{dt} = \left(\frac{e^{(V+50)/15} + e^{-(V+50)/16}}{30}\right)\left(\frac{1}{1+e^{(V+50)/7}} - h\right) \tag{2}$$

$$\frac{dn}{dt} = \left(\frac{e^{(V+40)/40} + e^{-(V+40)/50}}{7}\right)\left(\frac{1}{1+e^{-(V+23)/15}} - n\right) \tag{3}$$

$$\frac{du}{dt} = \frac{1}{75}\left(\frac{1}{1+e^{-(V+25)/3}} - u\right) \tag{4}$$

$$\frac{dr}{dt} = \left(\frac{e^{(V+140)/21.6} + e^{-(V+40)/22.7}}{6,000}\right)\left(\frac{1}{1+e^{(V+83.9)/7.4}} - r\right) \tag{5}$$

where V (mV), h, n, u, and r are state variables (V is the membrane potential of the vMN model, and h, n, u, and r are gating variables of ionic currents), t (ms) is time, I_{app} (μA/cm^2) is an external stimulation (in the present study, an I_{app} of 2.5 μA/cm^2 was applied to the vMN model between 1.0 s and 1.5 s, otherwise I_{app} was held zero.), g_{Na}, g_{AHP}, and g_h are maximal conductances of the transient sodium current, the AHP current, and the h-current, respectively. (Default values are $g_{Na} = 100.0$ mS/cm^2, $g_{AHP} = 10.0$ mS/cm^2, and $g_h = 0.05$ mS/cm^2. In the present study, these three conductance values were varied.).

The free and open source software Scilab (http://www.scilab.org/) was used to numerically solve the ODEs (initial conditions: $V = -65.84$ mV, $h = 0.92141213$, $n = 0.0497938$, $u = 0.00040176$, $r = 0.095137881$).

3. Results

First, the effect of variations in g_{Na} and g_{AHP} on the response of the vMN model to an external stimulation was examined. **Figure 1(a)** shows the time course of the membrane potential under conditions in which both g_{Na} and g_{AHP} are at default values. Before stimulation, the membrane potential was in a steady state (we define this state as the "down state"). During stimulation, repetitive spiking appeared. After the stimulation, the membrane potential recovered to the pre-stimulation level. **Figure 1(b)** shows the time course of the membrane potential under conditions in which g_{Na} is at default value but g_{AHP} is zero. The time course of the membrane potential was similar to that shown in **Figure 1(a)**. A remarkable difference between **Figure 1(a)** and 1B was that the frequency of repetitive spiking shown in **Figure 1(b)** was much larger than that shown in **Figure 1(a)**. **Figure 1(c)** shows the time course of the membrane potential under conditions in which g_{Na} is zero but g_{AHP} is at default value. The state of the membrane potential both before and after the stimulation was similar to those shown in **Figure 1(a)** and **Figure 1(b)**. In contrast, during the stimulation, although the membrane potential slightly depolarized, repetitive spiking did not occur. **Figure 1(d)** shows the time course of the membrane potential under conditions wherein both g_{Na} and g_{AHP} are zero. The state of the membrane potential before the stimulation was similar to that shown in **Figures 1(a)-(c)**. The state of the membrane potential during the stimulation was similar to that shown in **Figure 1(c)**. Interestingly, in contrast to **Figures 1(a)-(c)**, after the stimulation, the membrane potential did not return to the pre-stimulation level but instead stabilized at a slightly depolarized steady state
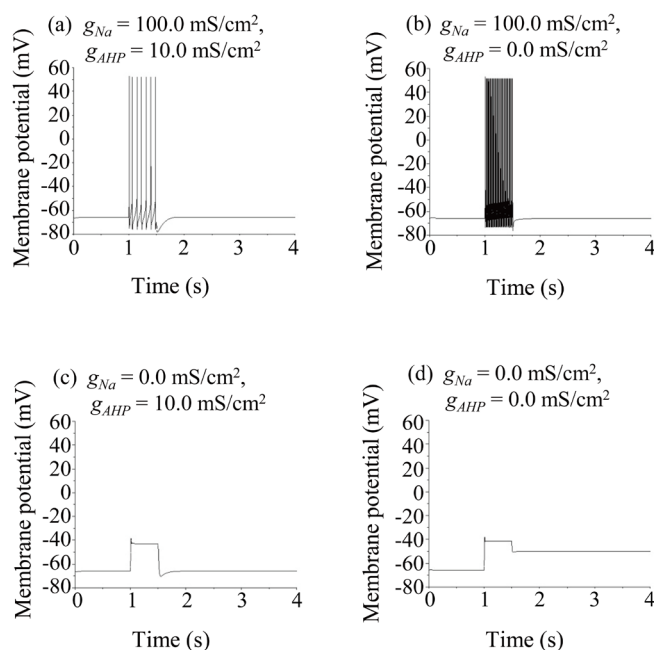

Figure 1. Time courses of the membrane potential of the vMN model at different values of g_{Na} and g_{AHP}. (a) (g_{Na}, g_{AHP}) = (100.0, 10.0); (b) (g_{Na}, g_{AHP}) = (100.0, 0.0); (c) (g_{Na}, g_{AHP}) = (0.0, 10.0); (d) (g_{Na}, g_{AHP}) = (0.0, 0.0). Throughout (a) to (d), g_h was held at 0.05 mS/cm^2.

(we define this state as the "up state") which continued even in the absence of an external stimulation.

Next, the effect of variations in g_{Na} and g_h on the response of the vMN model to an external stimulation was examined (**Figure 2**). Under conditions wherein both g_{Na} and g_h were at default values, the time course of the membrane potential was the same as that shown in **Figure 1(a)** (**Figure 2(a)**). A tendency similar to that shown in **Figure 2(a)** was observed under conditions wherein g_{Na} was at default value but g_h was zero (**Figure 2(b)**). Under conditions in which g_{Na} was zero but g_h was at default value, the time course of the membrane potential was the same as that shown in **Figure 1(c)** (**Figure 2(c)**). When both g_{Na} and g_h were zero, a similar pattern as in **Figure 2(c)** was observed (**Figure 2(d)**). A remarkable difference between **Figure 1** and **Figure 2** is that when g_{Na} was zero, the up state appeared under conditions in which g_{AHP} was zero but not under conditions in which g_h was zero (compare **Figure 1(d)** and **Figure 2(d)**).

Since **Figure 1(d)** indicates that the elimination of both g_{Na} and g_{AHP} plays an important role in inducing the stimulation-induced transition from the down state to the up state, we performed numerical simulation further focusing on the relationship between the transition and the levels of these two conductances in detail. We systematically varied the values of g_{Na} and g_{AHP} and investigated whether the transition had occurred or not (**Figure 3**). When g_{Na} was relatively large (e.g., $g_{Na} = 5.0$ mS/cm^2), the transition did not occur irrespective of the g_{AHP} value. Similarly, when g_{AHP} was relatively large (e.g., $g_{AHP} = 0.4$ or 0.5 mS/cm^2), the transition did not occur irrespective of the g_{Na} value. In other words, for the transition to occur, it is necessary (but not sufficient) to satisfy two conditions simultaneously: (1) g_{Na} was 4.0 mS/cm^2 or less and (2) g_{AHP} was 0.3 mS/cm^2 or less. When g_{Na} was between 2.0 and 4.0 mS/cm^2, the g_{AHP} range in which the transition occurred was $0.0 - 0.3$ mS/cm^2. When g_{Na} was between 0.0 and 1.0 mS/cm^2, the g_{AHP} range in which the transition occurred was $0.0 - 0.2$ mS/cm^2.

4. Discussion

The present study varied the values of g_{Na}, g_{AHP}, and g_h of the vMN model to reveal the effect of variations in these values on the response of the vMN model to an external stimulation. In particular, by appropriately modulating the values of g_{Na} and g_{AHP} (e.g., **Figure 1(d)** and **Figure 3**), a transiently applied external stimulation can transform the dynamical state of the vMN model from the down state to the up state. This indicates that under certain conditions, the vMN model can show bistability between the up and down states, which has not been re-
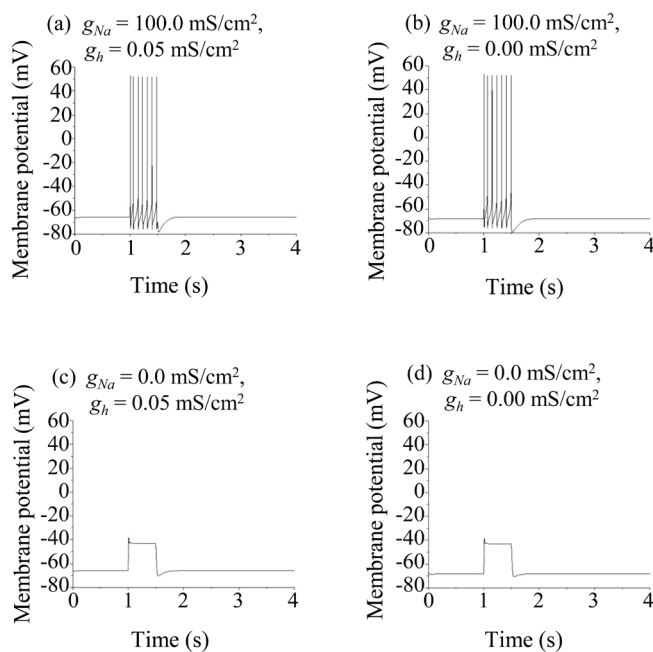

Figure 2. Time courses of the membrane potential of the vMN model at different values of g_{Na} and g_h. (a) $(g_{Na}, g_h) = (100.0, 0.05)$; (b) $(g_{Na}, g_h) = (100.0, 0.00)$; (c) $(g_{Na}, g_h) = (0.0, 0.05)$; (d) $(g_{Na}, g_h) = (0.0, 0.00)$. Throughout (a) to (d), g_{AHP} was held at 10.0 mS/cm^2.
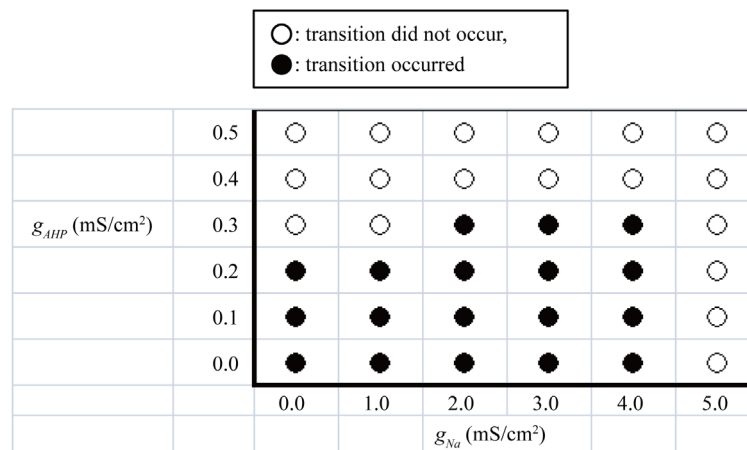
○: transition did not occur,
●: transition occurred

g_{AHP} (mS/cm²)		0.0	1.0	2.0	3.0	4.0	5.0
	0.5	○	○	○	○	○	○
	0.4	○	○	○	○	○	○
	0.3	○	○	●	●	●	○
	0.2	●	●	●	●	●	○
	0.1	●	●	●	●	●	○
	0.0	●	●	●	●	●	○
		0.0	1.0	2.0	3.0	4.0	5.0

g_{Na} (mS/cm²)

Figure 3. The dependence of the stimulation-triggered transition from a down state to an up state on g_{Na} and g_{AHP}. ○: the transition did not occur, ●: the transition occurred. g_h was held at 0.05 mS/cm².

ported in previous studies of the vMN model. Although previous studies have indicated that the vMN model shows bistability under certain conditions, it is different from the bistability described in the present study as it is the bistability between the resting and spiking states [3].

Previous studies of various types of mathematical neuron models have shown various types of bistability. Several examples have been reported: (1) bistability between periodic spiking and bursting states [10]-[12]; (2) bistability between period-2 spiking and bursting states [13]; (3) bistability between period-4 spiking and bursting states [13]; (4) bistability between chaotic spiking and bursting states [14] [15]; (5) bistability between two period-1 spiking states [16]; (6) bistability between period-1 spiking and period-2 spiking states [16]; (7) bistability between period-1 spiking and period-4 spiking states [16]; (8) bistability between period-1 spiking and chaotic spiking states [16]; (9) bistability between resting and spiking states [3] [7] [12]; and (10) bistability between resting and bursting states [12] [17]. Here, we consider a simple classification of bistability into three types: (a) bistability between oscillatory and steady states; (b) bistability between two oscillatory states; and (c) bistability between two steady states. Based on this classification scheme, the bistabilities from (1) to (8) correspond to type (b) and those from (9) and (10) correspond to the type (a); however, we cannot find type (c) within the bistabilities (1) to (10). The bistability revealed in the present study, which is bistability between the up and down states, is classified as type (c).

The present study indicates that simultaneous variations in ionic conductance values are useful for understanding the relationship between ionic conductances and the dynamical behavior of neuron models. The transition from the down state to the up state, which is described in the present study (**Figure 1** and **Figure 3**), was observed by simultaneously modulating both g_{Na} and g_{AHP}, while the modulation of neither g_{Na} alone nor g_{AHP} alone can induce the transition. In other words, the present results reveal that a simultaneous decrease in g_{Na} and g_{AHP} plays an important role in inducing a transition from the down state to the up state. The effect of the cooperation between different ionic conductances on the dynamical behavior of neuron models has also been described in a previous report: under certain conditions, neither a decrease in g_{Na} alone nor a decrease in g_{Ca} alone cannot stop pacemaking in a dopaminergic neuron model, but a simultaneous decrease in both g_{Na} and g_{Ca} can [5]. However, the combination of ionic conductances involved in the cooperative effect is different between the present (**Figure 1** and **Figure 3**) and the previous studies [5].

5. Conclusion

The following are the important findings of the present study: (1) under certain conditions, the vMN model can change the dynamical state from the down state to the up state in response to a transient external perturbation, which is a novel type of bistability that was not described in previous studies of the vMN model and (2) the change from the down state to the up state is induced by a simultaneous decrease in g_{Na} and in g_{AHP}. The present study contributes to an in-depth understanding of the relationship between ionic conductances and the dynamical

behavior of the vMN model.

Acknowledgements

References

[1] Ermentrout, G.B. and Terman, D. (2010) Mathematical Foundations of Neuroscience (Interdisciplinary Applied Mathematics). Springer, New York. http://dx.doi.org/10.1007/978-0-387-87708-2

[2] Harish, O. and Golomb, D. (2010) Control of the Firing Patterns of Vibrissa Motoneurons by Modulatory and Phasic Synaptic Inputs: A Modeling Study. *Journal of Neurophysiology*, **103**, 2684-2699. http://dx.doi.org/10.1152/jn.01016.2009

[3] Golomb, D. (2014) Mechanism and Function of Mixed-Mode Oscillations in Vibrissa Motoneurons. *PLoS ONE*, **9**, Article ID: e109205. http://dx.doi.org/10.1371/journal.pone.0109205

[4] Shirahata, T. (2015) Numerical Study of a Mathematical Model of Vibrissa Motoneurons: The Relationship between Repetitive Spiking and Two Types of Sodium Conductance. *International Journal of Theoretical and Mathematical Physics*, **5**, 48-52.

[5] Drion, G., Massotte, L., Sepulchre, R. and Seutin, V. (2011) How Modeling Can Reconcile Apparently Discrepant Experimental Results: The Case of Pacemaking in Dopaminergic Neurons. *PLoS Computational Biology*, **7**, Article ID: e1002050. http://dx.doi.org/10.1371/journal.pcbi.1002050

[6] Shirahata, T. (2011) The Effect of Variations in Sodium Conductances on Pacemaking in a Dopaminergic Retinal Neuron Model. *Acta Biologica Hungarica*, **62**, 211-214. http://dx.doi.org/10.1556/ABiol.62.2011.2.11

[7] Shirahata, T. (2014) Effect of Sodium Conductance Variations on Electrical Behavior of a Neocortical Neuron Model. *Acta Biologica Hungarica*, **65**, 379-384. http://dx.doi.org/10.1556/ABiol.65.2014.4.2

[8] Shirahata, T. (2015) Numerical Simulation Analysis of a Mathematical Model of Circadian Pacemaker Neurons. *Applied Mathematics*, **6**, 1214-1219. http://dx.doi.org/10.4236/am.2015.68113

[9] Shirahata, T. (2016) Quantitative Evaluations of the Contribution of the Excitatory Ionic Conductances to Repetitive Spiking in a Mathematical Model of Medial Vestibular Nucleus Neurons. *Acta Biologica Hungarica*, **67**, 215-219. http://dx.doi.org/10.1556/018.67.2016.2.9

[10] Komendantov, A.O. and Kononenko, N.I. (1998) Nonlinear Dynamics and Information Processing in Pacemaker Neurons. *Neurophysiology*, **30**, 330-333. http://dx.doi.org/10.1007/BF02462850

[11] Shilnikov, A., Calabrese, R.L. and Cymbalyuk, G. (2005) Mechanism of Bistability: Tonic Spiking and Bursting in a Neuron Model. *Physical Review E*, **71**, 056214. http://dx.doi.org/10.1103/PhysRevE.71.056214

[12] Shilnikov, A. (2012) Complete Dynamical Analysis of a Neuron Model. *Nonlinear Dynamics*, **68**, 305-328. http://dx.doi.org/10.1007/s11071-011-0046-y

[13] Shirahata, T. (2013) Novel Types of Bistability in a Model of a Bursting Pacemaker Neuron RPa1 from the Snail. *Helix pomatia*. *Acta Biologica Hungarica*, **64**, 131-135. http://dx.doi.org/10.1556/ABiol.64.2013.1.12

[14] Komendantov, A.O. and Kononenko, N.I. (1996) Deterministic Chaos in Mathematical Model of Pacemaker Activity in Bursting Neurons of Snail. *Helix pomatia*. *Journal of Theoretical Biology*, **183**, 219-230. http://dx.doi.org/10.1006/jtbi.1996.0215

[15] Shirahata, T. (2015) Numerical Simulation of Bistability between Regular Bursting and Chaotic Spiking in a Mathematical Model of Snail Neurons. *International Journal of Theoretical and Mathematical Physics*, **5**, 145-150.

[16] Cymbalyuk, G. and Shilnikov, A. (2005) Coexistence of Tonic Spiking Oscillations in a Leech Neuron Model. *Journal of Computational Neuroscience*, **18**, 255-263. http://dx.doi.org/10.1007/s10827-005-0354-7

[17] Barnett, W., O'Brien, G. and Cymbalyuk, G. (2013) Bistability of Silence and Seizure-Like Bursting. *Journal of Neuroscience Methods*, **220**, 179-189. http://dx.doi.org/10.1016/j.jneumeth.2013.08.021